

Effects of 3 MeV Proton Irradiation on Superconductivity and CDW in $2H\text{-NbSe}_2$ Single Crystals

Wenjie Li*, Sunseng Pyon, Akiyoshi Yagi, Tong Ren, Masahiro Suyama, Jiachen Wang, Takumi Matsumae, Yuto Kobayashi, Ayumu Takahashi, Daisuke Miyawaki, and Tsuyoshi Tamegai

Department of Applied Physics, The University of Tokyo, 7-3-1 Hongo, Bunkyo-ku, Tokyo 113-8656, Japan

Interplay between superconductivity and charge-density wave (CDW) in $2H\text{-NbSe}_2$ single crystals irradiated by 3 MeV protons is studied. Both T_c and T_{CDW} are found to decrease monotonically with the increase in irradiation dose. This behavior is different from electron-irradiated NbSe_2 , where T_{CDW} is suppressed monotonically with the increase in dose, while T_c shows an initial enhancement before it starts to decrease. We attempt to explain this difference based on the *negative pressure* effect which has been reported in our previous study on NbSe_2 irradiated by heavy ions.

1. Introduction

Artificial defects introduced by particle irradiations can act as pair-breakers and suppress T_c of superconductors [1-5]. However, the irradiation can also enhance T_c in superconductors with competing ground states (such as charge-density wave, CDW) [6-7]. One explanation for such T_c enhancement is based on the fact that superconductivity and CDW occur by using different parts of the Fermi surface. After the particle irradiation, CDW is suppressed and parts of the gapped Fermi surface will be released, which can be used to enhance the superconductivity. The competition between superconductivity and CDW has been observed in high-temperature cuprate superconductors [8-12], Kagome superconductor CsV_3Sb_5 [13-16], and low-temperature superconductors such as $\text{Lu}_5\text{Ir}_4\text{Si}_{10}$ [7] and NbSe_2 [6, 17-19]. Modifications of electronic states either by chemical doping or by physical pressure are typical methods which are usually used to study the relationship between superconductivity and CDW. Recently, the third method has been applied to the study of competition between superconductivity and CDW in terms of irradiation [6]. However, the results obtained by these methods are different in NbSe_2 . For the experiments using hydrostatic pressure [17-18] and electron irradiation [6] on NbSe_2 single crystals, with increasing pressure or irradiation

dose, T_c shows an initial enhancement, and after T_c reaching a maximum value it starts to decrease monotonically. In the case of hydrostatic pressure experiments, T_c can be enhanced from 7.2 K up to ~ 8.5 K [17-18]. In the case of 2.5 MeV electron irradiation, T_c has been enhanced from 7.25 K to ~ 7.45 K [6], followed by monotonic suppression by further increase in irradiation dose. On the other hand, through Te substitution into Se site in NbSe₂, T_c is monotonically decreased along with a monotonic enhancement of T_{CDW} [19]. All these results make it difficult to claim how superconductivity and CDW influence to each other in NbSe₂. So it is necessary to study the interplay between superconductivity and CDW in NbSe₂ in more detail.

In this paper, the interplay between superconductivity and CDW in NbSe₂ is studied by introducing artificial defects through 3 MeV proton irradiation. We followed the evolution of temperature dependence of resistivity via *in situ* resistivity measurements between successive irradiations, which are followed by the inspection of the crystal lattice with increasing dose.

2. Experimental Details

Single crystals of 2H-NbSe₂ were prepared by iodine vapor transport method as described in Ref. [20]. 3 MeV proton irradiation experiments were conducted at NIRS-HIMAC in Chiba, Japan. Before the irradiation, single crystals were prepared into thin plates with thickness of ~ 20 μm , which is thinner than the projected range of 3 MeV protons in NbSe₂ (~ 53 μm). The projected range is calculated by the stopping and range of ions in matter (SRIM-2008) [21]. For *in situ* resistivity measurements, gold wires with diameter of 25 μm were attached on the surface of the sample by silver paste in a standard four-probe configuration. After the sample was loaded onto a sapphire plate, the single crystal was cooled down by a closed-cycle refrigerator at the end of the irradiation port. The surface without gold wires was irradiated by protons. Irradiation was performed at 40 K to avoid annealing of created defects. The in-plane resistivity was measured by using both AC resistance bridge (LR-700, Linear Research) and DC nanovoltmeter (2182A, Keithley) with excitation current of 2 mA. The crystal structure was characterized at room temperature by using a commercial diffractometer (Smartlab, Rigaku) with Cu $K\alpha$ radiation. After determining diffraction angles, Bragg's law was used to calculate corresponding d -spacings, which are related to lattice parameters a and c by the relation for hexagonal lattice of

$$\frac{1}{d^2} = \frac{4(h^2 + hk + k^2)}{3a^2} + \frac{l^2}{c^2}, \quad (1)$$

where h , k , and l are Miller indices. In general, the Bragg peaks other than (00 l) peaks cannot

be directly obtained by using standard ω - 2θ scan for single crystals (ω is the sample angle and 2θ is the detector angle). According to the Laue condition for the constructive interference of

$$\Delta\mathbf{k} = \mathbf{k}_{\text{out}} - \mathbf{k}_{\text{in}} = \mathbf{G}, \quad (2)$$

where \mathbf{k}_{out} , \mathbf{k}_{in} , and \mathbf{G} are outgoing wave vector, incoming wave vector, and reciprocal lattice vector, respectively. ($h0l$) reciprocal lattice points can be brought onto the Ewald sphere by rotating the sample. Through successive optimizations of ω and 2θ , we can determine 2θ for ($10\bar{1}0$) peaks, from which we can determine d -spacing for ($10\bar{1}0$) plane. The c lattice parameter is calculated by taking an average value from (004), (006), and (008) peaks. For the calculation of a lattice parameter, the average value was taken from the observed six equivalent ($10\bar{1}0$) peaks. The magnetization measurements were conducted by using a commercial SQUID magnetometer (MPMS-XL5, Quantum Design).

3. Results and Discussion

3.1 In situ resistivity measurements

Based on the previous studies on the CDW in NbSe₂ [22-23], the CDW transition in NbSe₂ single crystal is relatively weak and the sample quality has strong influence on the formation of CDW. Thus, it is important to choose high-quality samples with low residual resistivity for the experiments. For that purpose, pristine samples used here have relatively large residual resistivity ratios $\text{RRR} \equiv \rho(300\text{ K})/\rho(8\text{ K}) \sim 50$. The CDW transition can be clearly observed at $T = 33\text{ K}$ in the pristine sample as shown in Fig. 1(a). With increasing proton dose, resistivity increases monotonically due to the effect of introduced artificial defects. Figure 1(b) is the enlarged temperature dependence of resistivity with increasing dose near T_c , where monotonic suppression of T_c can be clearly observed. To clearly identify the CDW transition, the temperature derivative of ρ , $d\rho/dT$, around the CDW transition is calculated as shown in Fig. 1(c). We define T_{CDW} as the local minimum of $d\rho/dT - T$ curves marked by arrows in Fig. 1(c). It is clear that T_{CDW} decreases monotonically with the increase in irradiation dose and it cannot be defined at the irradiation dose of $6 \times 10^{16}/\text{cm}^2$ or more. Figures 1(d) and (e) show evolution of T_{CDW} and T_c with increasing dose. Here, to make the quantitative comparison with electron irradiation [6] easy, the dose is replaced by the change in resistivity at $T = 40\text{ K}$, $\Delta\rho(40\text{ K})$. When the CDW is formed, the resistivity value below T_{CDW} should be enhanced compared with the putative value without CDW. This feature can provide an alternative way to identify the presence of CDW. In other words, difference in resistivity changes due to irradiation at the temperature above T_{CDW} and just above T_c can be a measure of CDW order. Actually, as shown in Fig. 1(f), $\Delta\rho(8\text{ K}) - \Delta\rho(40\text{ K})$ changes monotonically as CDW is suppressed by proton irradiation, and it saturates at a disorder level with $\Delta\rho(40\text{ K}) \sim 10\ \mu\Omega\cdot\text{cm}$, above which CDW is not observed any more as seen in Fig. 1(d). Very similar

behavior of $\Delta\rho$ (7.6 K) – $\Delta\rho$ (40 K) has also been reported in electron-irradiated NbSe₂ [6]. However, it should be noted that the increasing trend for $\Delta\rho$ (8 K) – $\Delta\rho$ (40 K) with disorder is opposite to what is expected for a system with CDW. Let us consider a system with two metallic bands, band 1 forming CDW (ρ_1 : red line) and band 2 responsible for superconductivity (ρ_2 : blue line) as shown in the inset of Fig. 1(f). For simplicity, we assume that band 1 turns into an insulator with infinite resistivity below T_{CDW} and the total resistivity of the system can be approximated by a parallel circuit of the two bands. In such a case, total resistivity should behave as shown by the black line (ρ_0) in the inset of Fig. 1(f). After complete suppression of CDW by irradiation-induced disorder, both bands should show metallic conduction with enhanced resistivity due to disorder (ρ_1' : broken red line and ρ_2' : broken blue line). Hence, the total resistivity after the suppression of CDW (ρ_0') should behave as shown by the broken black line in the inset of Fig. 1(f). Now it is clear that $\Delta\rho_a \equiv \Delta\rho$ (8 K) is smaller than $\Delta\rho_a \equiv \Delta\rho$ (40 K), making $\Delta\rho$ (8 K) – $\Delta\rho$ (40K) negative. Obviously, this decreasing trend of $\Delta\rho$ (8 K) – $\Delta\rho$ (40 K) with disorder is opposite to what we have observed experimentally. Such counter-intuitive behavior of resistivity at low temperatures with disorder in a system with CDW requires further detailed studies.

According to the Anderson theorem, nonmagnetic disorder will not affect T_c if a superconductor has an isotropic *s*-wave gap structure [24]. For NbSe₂, the anisotropic *s*-wave gap has been reported by thermal transport [25], angle-resolved photoemission spectroscopy [26], and scanning tunneling microscope measurements [27]. This means that the nonmagnetic disorder can act as pair-breaker and affect the T_c of NbSe₂. To discuss the pair-breaking effect due to nonmagnetic scattering quantitatively, we estimated the normalized scattering rate (*g*). *g* can be calculated based on the Drude model,

$$g = \frac{\hbar}{2\pi k_B T_{c0} \tau}, \quad (3)$$

where \hbar , k_B , and τ are the Planck's constant (divided by 2π), the Boltzmann constant, and the scattering time, respectively. In multi-gap superconductors, the scattering time includes at least two components, namely the interband scattering time τ_{inter} and intraband scattering time τ_{intra} . Both τ_{inter} and τ_{intra} play important roles to affect T_c and resistivity [28-29]. In the simplest case, if these two scattering times are the same, $\tau_{\text{inter}} = \tau_{\text{intra}} = \tau$,

$$\frac{1}{\Delta\rho_0} = \frac{1}{\Delta\rho_{\text{intra}}} + \frac{1}{\Delta\rho_{\text{inter}}} = \left(\frac{ne^2}{m^*} \right) (\tau_{\text{intra}} + \tau_{\text{inter}}) = \frac{2ne^2}{m^* \tau}. \quad (4)$$

By inserting Eq. (4) into Eq. (3), the normalized scattering rate can be calculated as

$$g = \frac{\hbar ne^2 \Delta\rho_0}{\pi k_B T_{c0} m^*}, \quad (5)$$

where n is the carrier density, $\Delta\rho_0 = \rho_0^i - \rho_0^0$ (the superscript i represents the i -th irradiation and the zero-temperature resistivity (ρ_0) was extrapolated through fitting the resistivity above

T_c to the function of $\rho = \rho_0 + aT^2$ (the dashed line in Fig. 1(a)), and m^* is the effective mass of the quasiparticle. Eq. (5) is only applicable to superconductors with multiple gap and equal scattering times. In the case of NbSe₂, its gap structure is still under debate. Evidences supporting two-gap feature have been reported in specific heat study [30], penetration depth measurement [31], pressure measurement [32], scanning tunneling spectroscopy [33], and quantum dot-assisted spectroscopy measurements [34]. There are also some experimental observations of single-gap with an anisotropic Fermi surface in NbSe₂ [35-36]. These debates make the accurate calculation of scattering rate g for NbSe₂ complicated. However, the purpose of our calculation of g is to compare the data on the effect of proton irradiation with the electron irradiation. So, for the sake of reasonable comparison, we choose the same treatment on g as in Ref. [37], where the interband scattering rate is considered to be 0. Thus, a factor of 1/2 should be multiplied in Eq. (4).

To simplify the calculation of g , the penetration depth $\lambda_0 = (m^*/\mu_0 ne^2)^{1/2}$ is used, which can allow us to avoid direct estimation of n and m^* . Then the formula for g , which is called g^λ , becomes

$$g^\lambda = \frac{\hbar\Delta\rho_0}{2\pi k_B T_{c0} \mu_0 \lambda^2}. \quad (6)$$

By using the penetration depth ($\lambda = 1250$ Å) of NbSe₂ reported in Ref. [31], the normalized T_c ($t_c = T/T_{c0}$) dependence of g^λ is plotted in Fig. 2. In Fig. 2, the curve for the suppression of T_c described by the Abrikosov-Gork'ov (AG) theory for magnetic pair-breaking is also included. AG theory can be described as

$$\ln(t_c) = \psi\left(\frac{1}{2} + \frac{g}{2t_c}\right) - \psi\left(\frac{1}{2}\right), \quad (7)$$

where ψ is the digamma function. As a reference, the data for NbSe₂ after 2.5 MeV electron irradiation [37] are also added. Except for the small g^λ range with complicated behavior in the case of electron irradiation, T_c suppression rate in NbSe₂ after proton irradiation (~ 0.03 K/ $\mu\Omega\cdot\text{cm}$) is smaller than that in electron irradiated crystals (~ 0.05 K/ $\mu\Omega\cdot\text{cm}$ [37]). This indicates that the defects introduced by proton irradiation act as weaker pair-breakers. One explanation for this difference is that the defects introduced by proton irradiation have larger dimension (cascade of point defects) than the defects introduced by electron irradiation (defects introduced by electron irradiation are mainly Frenkel pairs), the larger defects induce scattering with smaller wave numbers in reciprocal space, leading to weaker pair breaking.

Similar phenomena have also been observed in other superconductors. For example, by irradiating Ba_{1-x}K_xFe₂As₂ single crystals with 2.5 MeV electrons, T_c suppression rate is ~ 0.2

$\text{K}/\mu\Omega\cdot\text{cm}$ [5]. On the other hand, for $\text{Ba}_{1-x}\text{K}_x\text{Fe}_2\text{As}_2$ irradiated by 3 MeV protons, T_c suppression rate is weaker with suppression rate $\sim 0.1 \text{ K}/\mu\Omega\cdot\text{cm}$ [4]. In V_3Si single crystals, T_c suppression rate is $0.013 \text{ K}/\mu\Omega\cdot\text{cm}$ by 2.5 MeV electron irradiation [37], while it is $0.006 \text{ K}/\mu\Omega\cdot\text{cm}$ by 35 MeV proton irradiation [38]. These data suggested that defects introduced by electron irradiation act as stronger pair-breakers and affect T_c more than defects introduced by proton irradiation.

3.2 Expansion of lattice parameters

Materials in the ground state are expected in the state with the maximum density with minimum lattice parameters. It means that whenever defects are introduced by energetic particle irradiation, the crystal lattice is expected to expand to some extent. Actually, when materials are irradiated by heavy-ions, during the process of rapid cooling of the melted crystal amorphous tracks are created, which are known to have lower density with larger separation of constituent atoms. Due to the expansion of these amorphous regions, the surrounding lattice is forced to expand. Such lattice expansion has been observed in many materials after heavy-ion irradiations [20, 39-44]. In some superconductors, for example, the c -axis lattice parameter expansions have been observed at rates of $dT_c/dB_\Phi = 0.021\%/T$ (3.8 GeV Ta irradiation), $0.050\%/T$ (80 MeV I irradiation), $0.081\%/T$ (200 MeV I irradiation), and $0.163\%/T$ (120 MeV Au irradiation) on $\text{ErBa}_2\text{Cu}_3\text{O}_7$ thin films [43], where B_Φ is the dose equivalent matching field ($B_\Phi = 1 \text{ T}$ corresponds to $5 \times 10^{10}/\text{cm}^2$ defects). The lattice expansion has also been observed in our previous study on NbSe_2 single crystals after introducing columnar defects by heavy-ion irradiations, where the c -axis lattice parameters expanded at rates of $0.016\%/T$ (800 MeV Xe) and $0.030\%/T$ (320 MeV Au) [44]. Similarly, the lattice parameter expansion is also observed in NbSe_2 after 3 MeV proton irradiation in the present study.

Figures 3(a) and (b) show evolutions of (004) and $(10\bar{1}0)$ Bragg peaks with increasing irradiation dose for NbSe_2 single crystals, where Bragg peaks shift monotonically from higher angle to lower angle. The full width at half maximum (FWHM) in Figs. 3(c) and (d) show almost no change after 3 MeV proton irradiation, which indicates that the lattice expands uniformly by 3 MeV proton irradiation. As shown in Figs. 3(e) and (f), both c and a increase linearly at rates of $0.012\%/unit \text{ dose}$ and $0.011\%/unit \text{ dose}$ (unit dose equals $1 \times 10^{16}/\text{cm}^2$), respectively. Lattice parameters a and c are expanded at a similar rate after 3 MeV proton irradiation, which is different from the case of heavy-ion irradiations [44]. For NbSe_2

introduced with columnar defects by 320 MeV Au irradiation, expansion rate of the c -axis ($dc/dB_\Phi \sim 0.030\%/T$) is about twice larger than that of the a -axis ($da/dB_\Phi \sim 0.016\%/T$), at the same time, T_c was found to be suppressed almost linearly at a rate of 0.07 K/T [44]. It should be noted that the mechanism of lattice expansion by proton and heavy-ion is different. In the case of proton irradiation, the lattice change is mainly coming from the collision cascades between proton and target atom. In other words, the probability of a proton hitting the target atom is the same in different directions, which is consistent with the above results reporting a similar expansion rate for both a -axis and c -axis. On the other hand, heavy-ion irradiation creates separated linear amorphous tracks to expand lattice parameters, the effect for different direction should not be the same. In previous studies on Nb₃Sn irradiated by protons and heavier He ions, lattice parameter of the sample irradiated by He expanded more under the same irradiation dose; 0.005% [45] and 0.047% [46] at a dose of $1 \times 10^{16}/\text{cm}^2$ for proton and He, respectively. These results also suggest that the lattice expansion induced by irradiations of heavier ions is stronger.

3.3 T_c suppression after 3 MeV proton irradiation

Based on the above results, it is plausible that 3 MeV proton irradiation induces lattice expansion in NbSe₂ together with the monotonic suppression of T_c . In the study of hydrostatic pressure on NbSe₂ single crystals, T_c is enhanced with the shrinkage of lattice [47]. This means that T_c suppression and lattice expansion in NbSe₂ after 3 MeV proton irradiation can be considered as the effect of *negative pressure*. Figure 4(a) shows the dose dependence of T_c , which is estimated from the magnetization measurements as shown in the inset of Fig. 4(a). Monotonic decrease in T_c with increasing dose can be observed.

To accurately calculate how much T_c is suppressed by lattice expansion, it is necessary to separate the effect related to change in a -axis and in c -axis. For that purpose, the data for uniaxial pressure derivative of T_c along a -axis (dT_c/dp_a) and c -axis (dT_c/dp_c) are necessary. The hydrostatic pressure and the uniaxial pressure derivative of T_c are related by the formula of

$$\frac{dT_c}{dp} = 2 \frac{dT_c}{dp_a} + \frac{dT_c}{dp_c}. \quad (8)$$

By using reported data on dT_c/dp_c [48] and dT_c/dp [47] for NbSe₂ single crystals, dT_c/dp_a can be indirectly evaluated as $dT_c/dp_a = 0.10$ K/kbar. By combining the linear compressibilities ($\Delta a/a/\Delta p = 4.1 (\pm 0.4) \times 10^{-4}$ /kbar and $\Delta c/c/\Delta p = 16.2 (\pm 0.5) \times 10^{-4}$ /kbar [47]) of NbSe₂ with

the uniaxial pressure derivative of T_c for both a -axis and c -axis, the a -axis and c -axis lattice variation induced T_c changes are calculated as $dT_c/d(\Delta a/a) = -244$ K and $dT_c/d(\Delta c/c) = 91$ K. By connecting these data with the lattice expansion data for NbSe₂ irradiated by 3 MeV proton, T_c is expected to change -0.18 K by a -axis expansion and 0.07 K by c -axis expansion at a dose of $7 \times 10^{16}/\text{cm}^2$, resulting in a total T_c change of -0.29 K at this dose. This value is about ~46% of the experimental value of -0.63 K. As we mentioned above, factors which are known to affect T_c of NbSe₂ besides lattice expansion are disorder and CDW. For the effect of CDW on T_c in NbSe₂, how it quantitatively affects T_c is not yet clear. There are contradictory reports claiming enhancement [6, 17-18, 49] and suppression [50] of T_c by the destruction of CDW. T_c enhancement by the destruction of CDW can be understood based on the competition between superconductivity and CDW. On the other hand, T_c suppression by the destruction of CDW is explained based on the hardening of phonons leading to weaker electron-phonon interaction. According to the electron irradiation experiment on NbSe₂ [6], after CDW is completely destroyed by irradiation, T_c decreases almost linearly with the increase in irradiation dose. Based on the suppression rate of T_c at high dose ($dT_c/d\rho \sim 0.05$ K/ $\mu\Omega \cdot \text{cm}$) and assuming that this rate is independent of dose, we can estimate the T_c suppression induced by the corresponding disorder at the dose which forms the maximum T_c , and calculate how much T_c can be enhanced by the destruction of CDW as $|\Delta T (\text{CDW})| = |\Delta T (\text{disorder})| + |\Delta T (\text{measured value})|$. The $\Delta T (\text{CDW})$ at the maximum T_c in Ref. [6] is calculated to be 0.48 K ($|\Delta T (\text{disorder})| = |\Delta\rho| \times |dT_c/d\rho| = 0.28$ K, $|\Delta T (\text{measured value})| = 0.2$ K). We assume that this value also applies to the case of 3 MeV proton irradiation. With this assumption, the disorder-induced T_c suppression in NbSe₂ after 3 MeV proton irradiation can be estimated as $|\Delta T_c (\text{disorder})| = |\Delta T_c (\text{measured value})| - |\Delta T_c (\text{lattice expansion})| + |\Delta T_c (\text{CDW})|$. As an example, the disorder-induced T_c suppression for sample irradiated by 3 MeV proton irradiation with the dose of $7 \times 10^{16}/\text{cm}^2$ is calculated to be 0.63 K - 0.29 K + 0.48 K = 0.82 K. This result indicates that the T_c suppression induced by disorder is stronger than that of lattice expansion, which is different from the effect of columnar defects created by 320 MeV Au irradiation. In the case of 320 MeV Au irradiated NbSe₂ single crystals, the T_c suppression induced by lattice expansion is stronger than that by disorder [44].

Based on the above results, we may understand why the initial T_c enhancement is not observed in NbSe₂ single crystals irradiated by 3 MeV proton irradiation. Effects of proton irradiation on T_c can be divided into three factors, which are disorder, lattice expansion, and suppression of CDW as shown schematically in Fig. 4(b). At small proton irradiation doses, CDW is suppressed by disorder and the gapped Fermi surface is recovered. When CDW is

mostly suppressed at a critical dose Φ^* , T_c enhancement through this channel should stay constant above Φ^* . As a first approximation, we can assume that the change in T_c through this channel is a linear function of the dose below Φ^* . With the combination of all these three factors, T_c is expected to decrease monotonically as shown by the broken line in Fig. 4(b). As for the initial T_c enhancement observed in the electron irradiation experiments [6], there are two possible factors that may help us to understand it. The first is that the change in lattice parameters in electron irradiation for NbSe₂ may be ignored, since compared with the cascade point defects introduced by proton irradiation, the Frenkel pairs introduced by electron irradiation have a weaker effect on lattice parameters. Actually, we have performed XRD experiments on electron irradiated samples (some of 2.5 MeV electron irradiated NbSe₂ single crystals used in Ref. [6]) to observe the change in lattice parameters. In these measurements, no prominent lattice variations have been observed in samples irradiated with doses of 1.0 C and 1.6 C. Unfortunately, however, we cannot conclude that negligible lattice variation occurs in electron irradiated crystals, since the T_c of these crystals have returned almost to the pristine value due to long-term room temperature annealing. Another factor is the effect of CDW on T_c . As mentioned above, the effect of disorder on T_c in electron-irradiated sample is stronger than that in proton-irradiated samples. So if only the effects from CDW and disorder on T_c for electron irradiation are considered, the initial T_c enhancement should not be observed in NbSe₂ irradiated by electron. However, by comparing the dose dependence of T_{CDW} for electron irradiation and proton irradiation, we found that T_{CDW} is suppressed faster in electron irradiation [6] than proton irradiation. This fact may suggest that T_c enhancement by CDW is faster in the electron irradiated samples below Φ^* . If this is true, it is possible to observe an initial T_c enhancement by considering the effects of disorder and CDW in small electron irradiation dose. It is interesting to note that T_c in Nb_{1-x}Ta_xSe₂ with atomic scale disorder also show nonlinear initial enhancement of T_c [49].

4. Summary

We conducted *in situ* resistivity measurements on 2H-NbSe₂ single crystals irradiated by 3 MeV protons. Unlike the effects of 2.5 MeV electron irradiation on NbSe₂ single crystals, introduction of low-density point defects did not enhance superconductivity. Instead, both T_{CDW} and T_c were monotonically suppressed with the increase in irradiation dose. Weak but finite lattice expansions along both *a*-axis and *c*-axis were observed after the 3 MeV proton irradiation. By analyzing the lattice-expansion-induced T_c suppression based on the *negative pressure* effect with that based on disorder due to proton irradiation on NbSe₂, T_c was found to

be suppressed more by disorder rather than by lattice expansion. This is different from the effect of columnar defects on NbSe₂ single crystals. In addition, comparison of the T_c suppression rate after proton and electron irradiations, it turns out that defects introduced by proton irradiation in NbSe₂ act as weaker pair-breakers, which is consistent with the case for Ba_{1-x}K_xFe₂As₂ and V₃Si single crystals.

Acknowledgment

We would like to thank Prof. R. Prozorov for providing us the 2.5 MeV electron irradiated NbSe₂ single crystals for XRD experiments as well as illuminating discussions.

*E-mail: wenjiecd@gmail.com

- 1) Y. Sun, A. Park, S. Pyon, T. Tamegai, T. Kambara, and A. Ichinose, Phys. Rev. B **95**, 104514 (2017).
- 2) Y. Nakajima, T. Taen, Y. Tsuchiya, T. Tamegai, H. Kitamura, and T. Murakami, Phys. Rev. B **82**, 220504(R) (2010).
- 3) A. Park, S. Pyon, Y. Sun, I. Veshchunov, J. Chen, N. Ito, T. Suwa, and T. Tamegai, Phys. Rev. B **98**, 054512 (2018).
- 4) T. Taen, F. Ohtake, H. Akiyama, H. Inoue, Y. Sun, S. Pyon, and T. Tamegai, Phys. Rev. B **88**, 224514 (2013).
- 5) R. Prozorov, M. Kończykowski, M. A. Tanatar, A. Thaler, S. L. Bud'ko, P. C. Canfield, V. Mishra, and P. J. Hirschfeld, Phys. Rev. X **4**, 041032 (2014).
- 6) K. Cho, M. Konczykowski, S. Teknowijoyo, M. A. Tanatar, J. Guss, P. Gartin, J. M. Wilde, A. Kreyssig, R. McQueeney, A. I. Goldman, V. Mishra, P. J. Hirschfeld, and R. Prozorov, Nat. Commun. **9**, 2796 (2018).
- 7) M. Leroux, V. Mishra, C. Opagiste, P. Rodière, A. Kayani, W. Kwok, and U. Welp, Phys. Rev. B **102**, 094519 (2020).
- 8) J. Chang, E. Blackburn, A. T. Holmes, N. B. Christensen, J. Larsen, J. Mesot, R. Liang, D. A. Bonn, W. N. Hardy, A. Watenphul, M. V. Zimmermann, E. M. Forgan, and S. M. Hayden, Nat. Phys. **8**, 871 (2012).
- 9) D. H. Torchinsky, F. Mahmood, A. T. Bollinger, I. Bozovic, and N. Gedik, Nat. Mater. **12**, 387 (2013).
- 10) T. P. Croft, C. Lester, M. S. Senn, A. Bombardi, and S. M. Hayden, Phys. Rev. B **89**, 224513 (2014).
- 11) H. H. Kim, S. M. Souliou, M. E. Barber, E. Lefrançois, M. Minola, M. Tortora, R. Heid, N. Nandi, R. A. Borzi, G. Garbarino, A. Bosak, J. Porras, T. Loew, M. König, P. J. W. Moll, A. P. Mackenzie, B. Keimer, C. W. Hicks, and M. Le Tacon, Science **362**, 1040 (2018).
- 12) B. Loret, N. Auvray, Y. Gallais, M. Cazayous, A. Forget, D. Colson, M.-H. Julien, I. Paul,

- M. Civelli, and A. Sacuto, *Nat. Phys.* **15**, 771 (2019).
- 13) F. H. Yu, D. H. Ma, W. Z. Zhuo, S. Q. Liu, X. K. Wen, B. Lei, J. J. Ying, and X. H. Chen, *Nat. Commun.* **12**, 3645 (2021).
 - 14) Y. Song, T. Ying, X. Chen, X. Han, X. Wu, A. P. Schnyder, Y. Huang, J. Guo, and X. Chen, *Phys. Rev. Lett.* **127**, 237001 (2021).
 - 15) K. Y. Chen, N. N. Wang, Q. W. Yin, Y. H. Gu, K. Jiang, Z. J. Tu, C. S. Gong, Y. Uwatoko, J. P. Sun, H. C. Lei, J. P. Hu, and J. G. Cheng, *Phys. Rev. Lett.* **126**, 247001 (2021).
 - 16) T. Qian, M. H. Christensen, C. Hu, A. Saha, B. M. Andersen, R. M. Fernandes, T. Birol, and N. Ni, *Phys. Rev. B* **104**, 144506 (2021).
 - 17) O. Moulding, I. Osmond, F. Flicker, T. Muramatsu, and S. Friedemann, *Phys. Rev. Res.* **2**, 043392 (2020).
 - 18) A. Majumdar, D. VanGennep, J. Brisbois, D. Chareev, A. V. Sadakov, A. S. Usoltsev, M. Mito, A. V. Silhanek, T. Sarkar, A. Hassan, O. Karis, R. Ahuja, and M. Abdel-Hafiez, *Phys. Rev. Mater.* **4**, 084005 (2020).
 - 19) H. Wang, L. Li, D. Ye, X. Cheng, and Z. Xu, *Chinese Phys.* **16**, 2471 (2007).
 - 20) W. Li, S. Pyon, A. Takahashi, D. Miyawaki, Y. Kobayashi, and T. Tamegai, *J. Phys.: Conf. Ser.* **1590**, 012003 (2020).
 - 21) J. Ziegler, J. Biersack, and U. Littmark, *The Stopping and Range of Ions in Solids* (Pergamon, New York, 1985).
 - 22) K. Iwaya, T. Hanaguri, A. Koizumi, K. Takaki, A. Maeda, and K. Kitazawa, *Physica B* **329**, 1598 (2003).
 - 23) L. Li, Z. Xu, J. Shen, L. Qiu, and Z. Gan, *J. Phys.: Condens. Matter* **17**, 493 (2005).
 - 24) P. W. Anderson, *J. Phys. Chem. Solids* **11**, 26 (1959).
 - 25) E. Boaknin, M. A. Tanatar, J. Paglione, D. Hawthorn, F. Ronning, R. W. Hill, M. Sutherland, L. Taillefer, J. Sonier, S. M. Hayden, and J. W. Brill, *Phys. Rev. Lett.* **90**, 117003 (2003).
 - 26) T. Yokoya, T. Kiss, A. Chainani, S. Shin, M. Nohara, and H. Takagi, *Science* **294**, 2518 (2001).
 - 27) H. F. Hess, R. B. Robinson, and J. V. Waszczak, *Phys. Rev. Lett.* **64**, 2711 (1990).
 - 28) D. V. Efremov, M. M. Korshunov, O. V. Dolgov, A. A. Golubov, and P. J. Hirschfeld, *Phys. Rev. B* **84**, 180512 (2011).
 - 29) Y. Wang, A. Kreisel, P. J. Hirschfeld, and V. Mishra, *Phys. Rev. B* **87**, 094504 (2013).
 - 30) C. L. Huang, J.-Y. Lin, Y. T. Chang, C. P. Sun, H. Y. Shen, C. C. Chou, H. Berger, T. K. Lee, and H. D. Yang, *Phys. Rev. B* **76**, 212504 (2007).
 - 31) J. D. Fletcher, A. Carrington, P. Diener, P. Rodière, J. P. Brison, R. Prozorov, T. Olheiser, and R. W. Giannetta, *Phys. Rev. Lett.* **98**, 057003 (2007).
 - 32) H. Suderow, V. G. Tissen, J. P. Brison, J. L. Martí'nez, and S. Vieira, *Phys. Rev. Lett.* **95**, 117006 (2005).
 - 33) Y. Noat, J. A. Silva-Guill'en, T. Cren, V. Cherkez, C. Brun, S. Pons, F. Debontridder, D.

- Roditchev, W. Sacks, L. Cario, P. Ordejón, A. García, and E. Canadell, *Phys. Rev. B* **92**, 134510 (2015).
- 34) T. R. Devidas, I. Keren, and H. Steinberg, *Nano Lett.* **21**, 6931 (2021).
- 35) E. W. Scheidt, M. Herzinger, A. Fischer, D. Schmitz, J. Reiners, F. Mayr, F. Loder, M. Baenitz, and W. Scherer, *J. Phys.: Condens. Matter* **27**, 155701 (2015).
- 36) A. Sanna, C. Pellegrini, E. Liebhaber, K. Rossnagel, K. J. Franke, and E. K. U. Gross, *npj Quantum Mater.* **7**, 6 (2022).
- 37) K. Cho, M. Kończykowski, S. Ghimire, M. A. Tanatar, L. L. Wang, V. G. Kogan, and R. Prozorov, *Phys. Rev. B* **105**, 024506 (2022).
- 38) S. A. Alterovitz, D. E. Farrell, B. S. Chandrasekhar, E. J. Haugland, J. W. Blue, and D. C. Liu, *Phys. Rev. B* **24**, 90 (1981).
- 39) X. Fan, M. Terasawa, T. Mitamura, T. Kohara, K. Ueda, H. Tsubakino, A. Yamamoto, T. Murakami, and S. Matsumoto, *Nucl. Instrum. Methods Phys. Res. B* **121**, 331 (1997).
- 40) Y. Yamamoto, N. Ishikawa, F. Hori, and A. Iwase, *Quantum Beam Sci.* **4**, 26 (2020).
- 41) S. G. Jung, S. K. Son, D. Pham, W. C. Lim, J. Song, W. N. Kang, and T. Park, *Supercond. Sci. Technol.* **34**, 129501 (2021).
- 42) R. Biswal, J. John, P. Mallick, B. N. Dash, P. K. Kulriya, D. K. Avasthi, D. Kanjilal, D. Behera, T. Mohanty, P. Raychaudhuri, and N. C. Mishra, *J. Appl. Phys.* **106**, 053912 (2009).
- 43) A. Iwase, N. Ishikawa, Y. Chimi, K. Tsuru, H. Wakana, O. Michikami, and T. Kambara, *Nucl. Instrum. Methods Phys. Res. B* **557**, 146 (1998).
- 44) W. Li, S. Pyon, A. Ichinose, S. Okayasu, and T. Tamegai, *J. Phys. Soc. Jpn.* **91**, 074709 (2022).
- 45) A. I. Ryazanov, R. D. Svetogorov, Ya. V. Zubavichus, V. N. Unezhev, S. T. Latushkin, and E. V. Semenov, *Crystallogr. Rep.* **65**, 352 (2020).
- 46) R. Dynes, J. Poate, L. Testardi, A. Storm, and R. Hammond, *IEEE Trans. Magn.* **13**, 640 (1977).
- 47) R. E. Jones, H. R. Shanks, D. K. Finnemore, and B. Morosin, *Phys. Rev. B* **6**, 835 (1972).
- 48) T. Sambongi, *J. Low Temp. Phys.* **18**, 139 (1975).
- 49) B. J. Dalrymple, S. Mroczkowski, and D. E. Prober, *J. Cryst. Growth* **74**, 575 (1986).
- 50) F. Zheng and J. Feng, *Phys. Rev. B* **99**, 161119 (R) (2019).

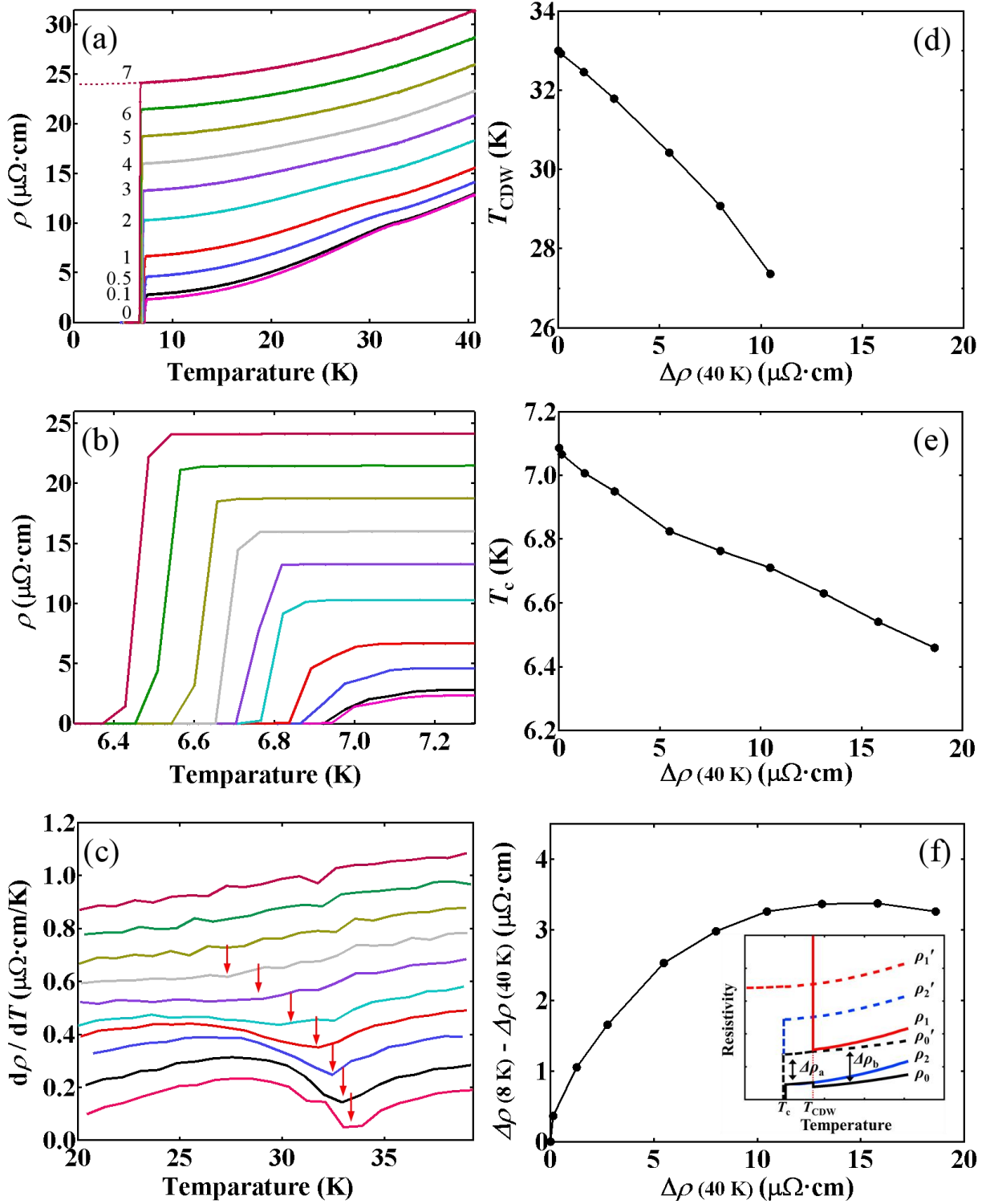


Fig. 1. (Color online) (a) *In situ* resistivity measurement results for NbSe₂ single crystal irradiated by 3 MeV protons up to a maximum dose of $7 \times 10^{16}/\text{cm}^2$. (b) The enlarged $\rho - T$ curves around T_c region. (c) The derivative of temperature dependence of resistivity. Disorder (evaluated by $\Delta\rho$ at 40 K) dependence of (d) T_{CDW} , (e) T_c , and (f) $\Delta\rho$ (8 K) - $\Delta\rho$ (40 K). The inset of (f) shows a schematic diagram of temperature dependence of resistivity for a system with two bands, band 1 forming CDW and band 2 responsible for superconductivity before and after the introduction of defects. Refer to the main text for definitions of all labels.

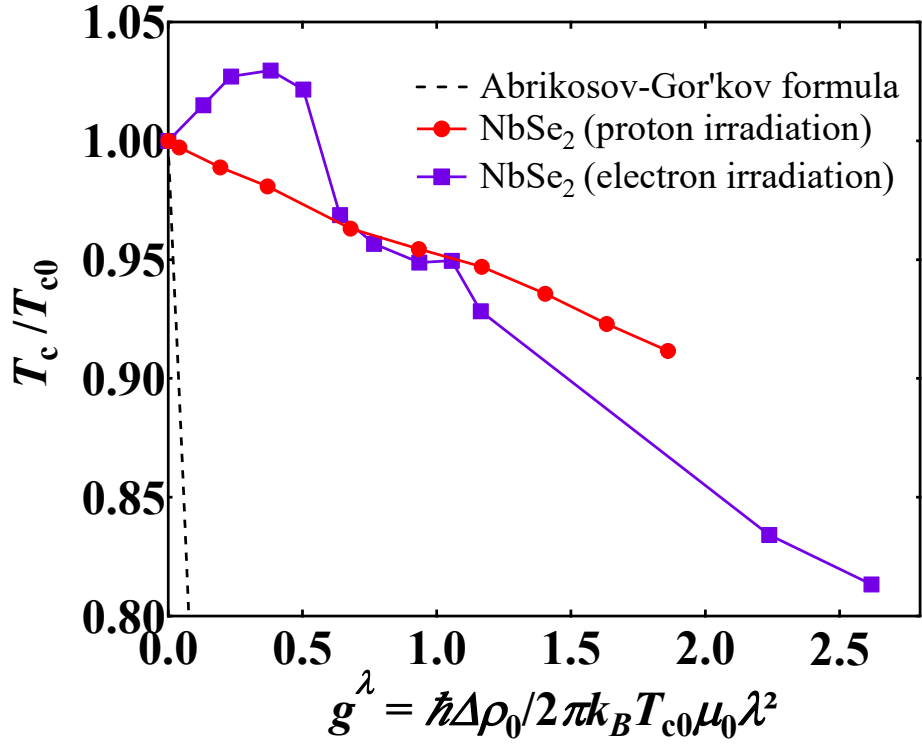


Fig. 2. (Color online) T_c/T_{c0} as a function of a normalized scattering rate in NbSe₂ single crystal irradiated by 3 MeV protons evaluated by London penetration depth $g^\lambda = \hbar\Delta\rho_0/(2\pi k_B T_{c0}\mu_0\lambda^2)$. Data for NbSe₂ single crystals irradiated by 2.5 MeV electrons is also included [37].

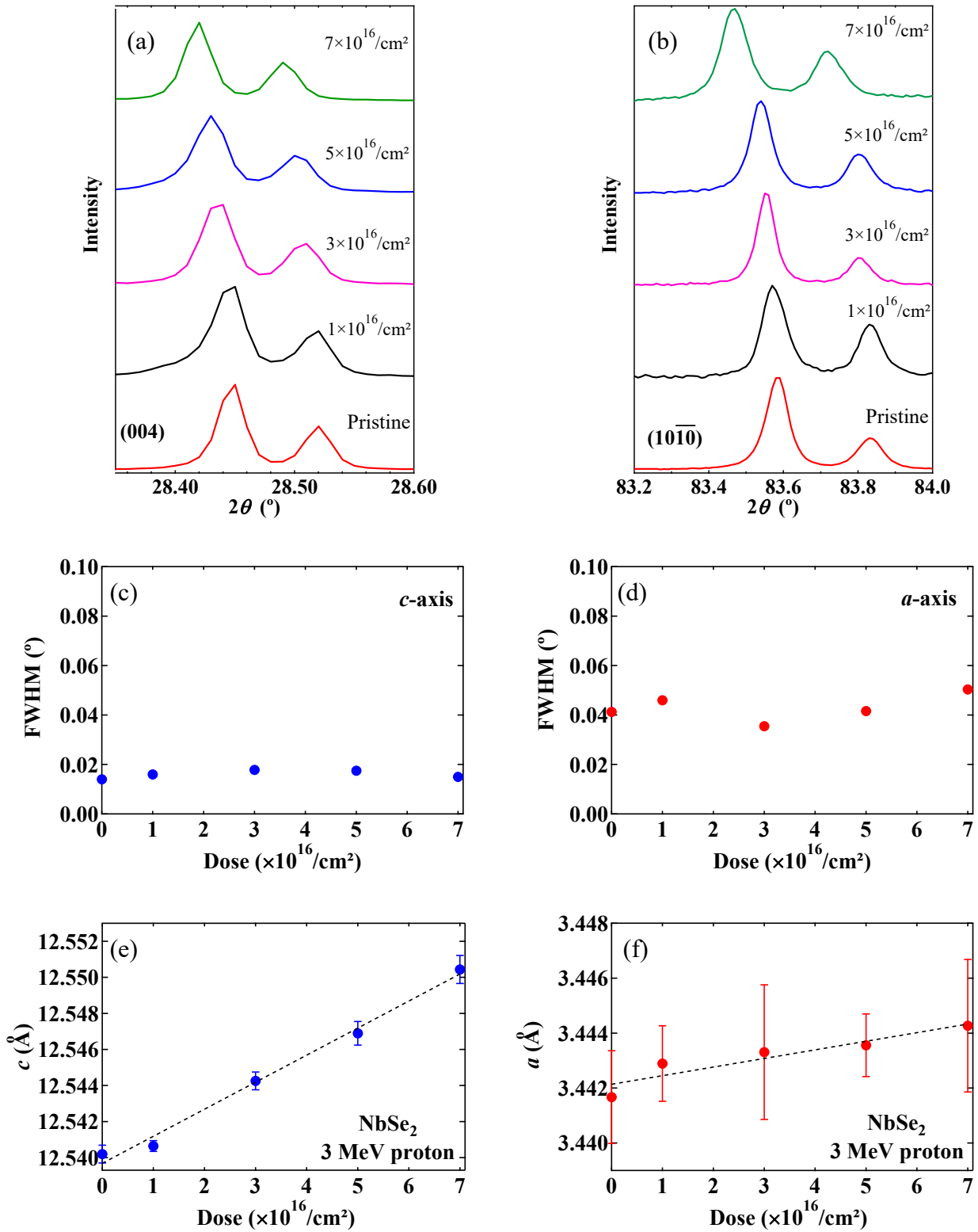


Fig. 3. (Color online) (a) (004) and (b) (10 $\bar{1}0$) diffraction peak profiles for NbSe₂ single crystals before and after 3 MeV proton irradiation. Dose dependences of FWHM of (c) (004) and (d) (10 $\bar{1}0$) peaks for NbSe₂ single crystals after 3 MeV proton irradiation. Dose dependences of (e) *c*-axis and (f) *a*-axis lattice parameters for NbSe₂ single crystals after 3 MeV proton irradiation.

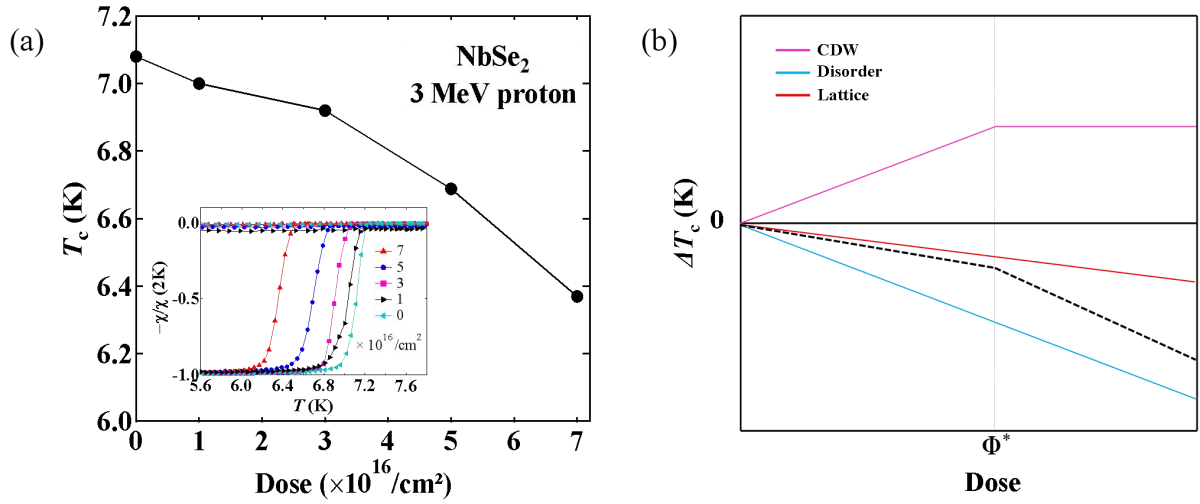


Fig. 4. (Color online) (a) The dose dependence of T_c for NbSe₂ single crystals before and after 3 MeV proton irradiation. T_c decreases monotonically with the increase in irradiation dose. The inset shows the temperature dependence of the normalized magnetic susceptibility for pristine and irradiated crystals. (b) Schematic changes of T_c in NbSe₂ induced by CDW, disorder, and lattice expansion. Φ^* is the critical dose where CDW is completely suppressed. The combination of the three factors results in the expected change in T_c (black dashed line) with increasing irradiation dose.